

MODELLING OF BRUSHLESS DC MOTOR USING PID, PWM AND CASCADED CONTROLLERS

S. Naga Santosh¹,

Dr. N. Prema Kumar²

¹Dept.of Electrical Engineering, Andhra University College of Engineering (A)
Visakhapatnam, Andhra Pradesh, India

²Dept.of Electrical Engineering, Andhra University College of Engineering (A)
Visakhapatnam, Andhra Pradesh, India

Abstract

The paper presents a model of three phase star connected brushless dc motor considering the behaviour of motor during commutation. This process is done in MATLAB/SIMULINK after development of the BLDC motor with sinusoidal and trapezoidal waveforms of back-EMF. A comparison study is presented between the MATLAB/SIMULINK models of sinusoidal and trapezoidal models of back-EMF.

Keywords: BLDC, MATLAB/SIMULINK, EMF.

I. INTRODUCTION

A motor that retains the characteristics of a dc motor but eliminates the commutator and the brushes is called a Brushless DC motor. BrushlessDC (bl dc) motors can in many cases replace conventional DC motors. They are driven by dc voltage but current commutation is done by solid state switches i.e., the commutation is done electronically. BLDC motors are available in many different power ratings, from very small motors as used in hard disk drives to large motors in electric vehicles. Three phase motors are most common but two phase motors are also found in many applications. The BLDC motors have many advantages over brushed DC motors. A few of these are:

- Higher speed ranges
- Higher efficiency
- Better speed versus torque characteristics
- Long operating life
- Noiseless operation
- Higher dynamic response

The torque of the BLDC motor is mainly influenced by the waveform of back-EMF (the voltage induced into the stator winding due to rotor movement). The ratio of torque delivered

to the size of the motor is higher, making it useful in applications where space and weight are critical factors. Ideally, the BLDC motors have trapezoidal back-EMF waveforms and are fed with rectangular stator currents, which give a theoretically constant torque. However, in practice, torque ripple exists, mainly due to emf waveform imperfections, current ripple and phase current commutation. The current ripple result is from PWM or hysteresis control. The emf waveform imperfections result from variations in the shapes of slot, skew and magnet of BLDC motor, and are subject to design purposes. Hence, an error can occur between actual value and the simulation results. This paper attempts to compare various types of BLDC motor models with the trapezoidal and sinusoidal back-EMF waveforms. The simple motor model of a BLDC motor consisting of a 3-phase power stage and a brushless DC motor is shown in Fig.1.

II. CONSTRUCTION AND OPERATING PRINCIPLE

The BLDC motor is also referred to as an electronically commutated motor. There are no brushes on the rotor and the commutation is performed electronically at certain rotor positions. The stator phase windings are inserted in the slots (a distributed winding), or can be wound as one coil on the magnetic pole. The magnetization of the permanent magnets and their displacement on the rotor are chosen in such a way that the back-EMF shape is trapezoidal. This allows the three-phase voltage system, with a rectangular shape, to be used to create a rotational field with low torque ripples. In this respect, the BLDC motor is equivalent to an inverted DC commutator motor in that the magnets rotate while the conductors remain stationary in that the magnets rotate while the conductors remain stationary.

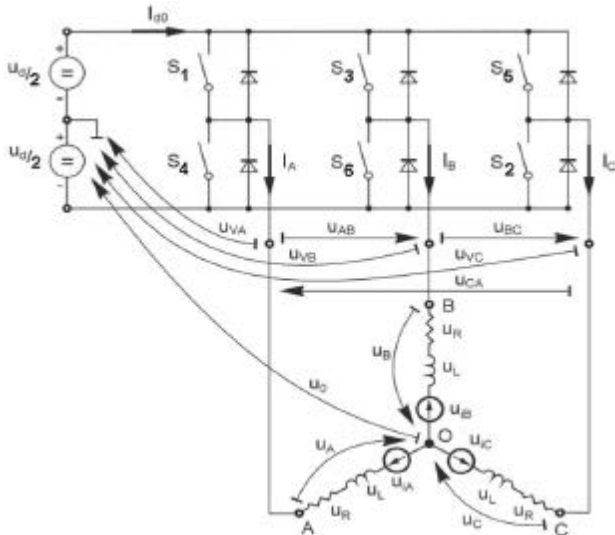


Fig.1. BLDC motor model of electrical circuits

In the DC commutator motor, the current polarity is reversed by the commutator and the brushes, but in the brushless DC motor, the polarity reversal is performed by semiconductor switches which are to be switched in synchronization with the rotor position. Besides the higher reliability, the missing commutator brings another advantage. The commutator is also a limiting factor in the maximal speed of the DC motor. Therefore the BLDC motor can be employed in applications requiring high speed. Replacement of a DC motor by a BLDC motor place higher demands on control algorithm and control circuit. Firstly, the BLDC motor is usually considered as a three-phase system. Thus, it has to be powered by a three-phase power supply. Next, the rotor position must be known at certain angles, in order to align the applied voltage with the back-EMF. The alignment between the back-EMF and commutation events is very important. In this condition the motor behaves as a DC motor and runs at the best working point. But the drawbacks of the BLDC motor caused by necessity of power converter and rotor position measurement are balanced by excellent performance and reliability, and also by the ever-falling prices of power components and control circuits.

III. Mathematical Model of the BLDC Motor

Modelling of a BLDC motor can be developed in the similar manner as a three-phase synchronous machine. Since there is a permanent magnet mounted on the rotor, some dynamic characteristics are different. Flux linkage from the rotor depends upon the magnet material. Therefore, saturation of magnetic flux is typical for this kind of motors. As any typical three-phase motors, one structure of the BLDC motor is fed by a three phase voltage source. The source is not necessarily to be sinusoidal. Square wave or other wave-shape can be applied as long as the peak voltage does not exceed the

maximum voltage limit of the motor. Similarly, the model of the armature winding for the BLDC motor is expressed as

$$V_a = R_{ia} + \frac{d i_a}{dt} \quad (1)$$

$$V_b = R_{ib} + \frac{d i_b}{dt} \quad (2)$$

$$V_c = R_{ic} + \frac{d i_c}{dt} \quad (3)$$

Where,

L is armature self-inductance [H], R-armature resistance [Ω], V_a, V_b, V_c – terminal phase voltage [V], i_a, i_b, i_c – motor input current [A], and e_a, e_b, e_c – motor back-EMF [V]. In the 3-phase BLDC motor, the back-EMF is related to a function of rotor position and the rotor position and the back-EMF of each phase has 120° phase angle difference so equation of each phase should be as follows: voltages of the stator and rotor windings can be expressed as the sum of the voltage drops in resistances, and rate of change of flux linkages, which are the products of currents and inductances. From the above figure the terminal voltages are as follows,

$$e_a = K \omega f(\theta_e) \quad (4)$$

$$e_b = K \omega f(\theta_e - 2\pi/3) \quad (5)$$

$$e_c = K \omega f(\theta_e + 2\pi/3) \quad (6)$$

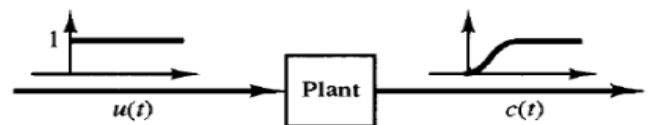
$$\theta_e = \frac{p}{2} \theta_m \quad (7)$$

Total torque output can be represented as summation of that of each phase. Next equation represents the total torque output:

$$T_e - T_l = J \frac{d\omega}{dt} + B\omega \quad (8)$$

IV. PID CONTROL THEORY

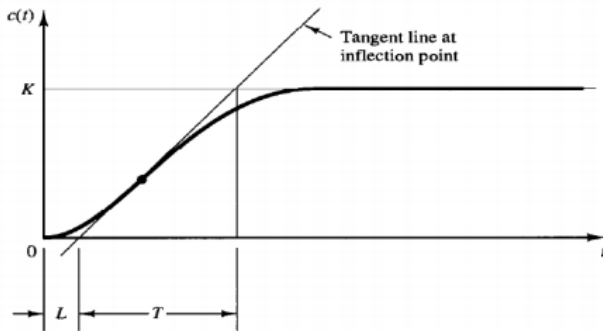
Zeigler-Nichols proposed rules for determining values of the proportional gain, integral time, and derivative time base on transient response characteristics of a given plant. Such determination of parameters of PID controllers can be made by engineers on site by experiments on plants. There are two methods of Ziegler Nichols tuning rules. In both the methods, they aimed at obtaining 25% maximum overshoot in step response. If the plant involves neither integrator(s) nor denominator complex conjugate poles, then such unit step response curve may look like an S-shaped curve, as shown. Such step response curves may be generated experimentally or from a dynamic simulation of the plant.



The S-shaped curve may be characterized by two constants, delay time L and time constant T. the delay time and time constant are determined by drawing a tangent line at the inflection point of the S-shaped curve and determining the intersections of the tangent line with the time axis and line $c(t) = K$. The transfer function $C(S)/U(S)$ may then be approximated by a first order system with a transport lag as follows

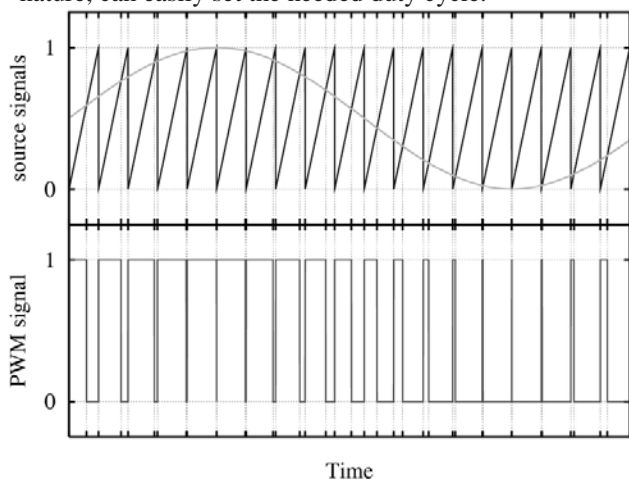
$$\frac{C(S)}{U(S)} = \frac{Ke^{-Ls}}{Ts + 1}$$

$$RiseTime = \frac{\pi - \tan^{-1} \sqrt{1-\zeta^2}}{\omega_n \sqrt{1-\zeta^2}}$$



V. PWM CONTROL

Pulse-width modulation (PWM), or pulse-duration modulation (PDM), is a modulation technique that controls the width of the pulse, formally the pulse duration, based on modulator signal information. Although this modulation technique can be used to encode information for transmission, its main use is to allow the control of the power supplied to electrical devices, especially to inertial loads such as motors. The average value of voltage (and current) fed to the load is controlled by turning the switch between supply and load on and off at a fast pace. The longer the switch is on compared to the off periods, the higher the power supplied to the load. The main advantage of PWM is that power loss in the switching devices is very low. When a switch is off there is practically no current, and when it is on, there is almost no voltage drop across the switch. Power loss, being the product of voltage and current, is thus in both cases close to zero. PWM also works well with digital controls, which, because of their on/off nature, can easily set the needed duty cycle.



Rise Time is the time taken by a signal to change from 0% and 100% of the step height for under damped system.

Peak Time is the time required for the response to reach the peak overshoot.

$$PeakTime = \frac{\pi}{\omega_n \sqrt{1-\zeta^2}}$$

Settling Time is the time required for the response to reach and stay at a specified tolerance band of its final value.

$$SettlingTime = \frac{\ln(\%error)}{\zeta \omega_n}$$

Peak Overshoot is normalized difference between the time responses peak and steady % is defined is

$$PeakOvershoot = \frac{C(Peak\ Response) - C(\infty)}{C(\infty)}$$

VI. Simulation and Results

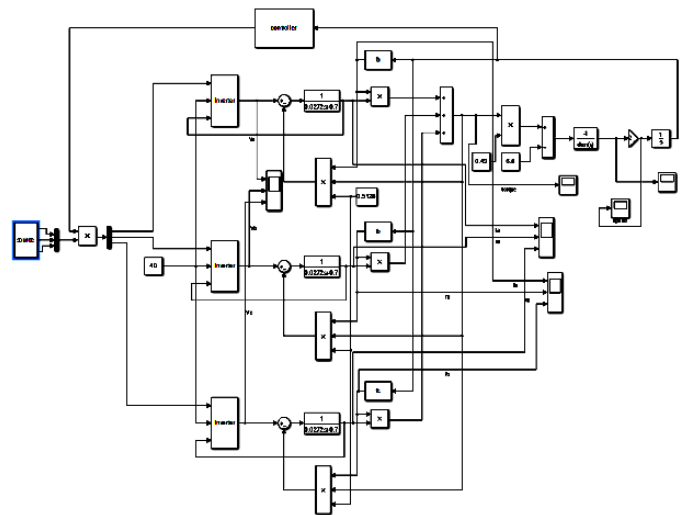


Fig.1 Block Diagram of BLD motor with Controller

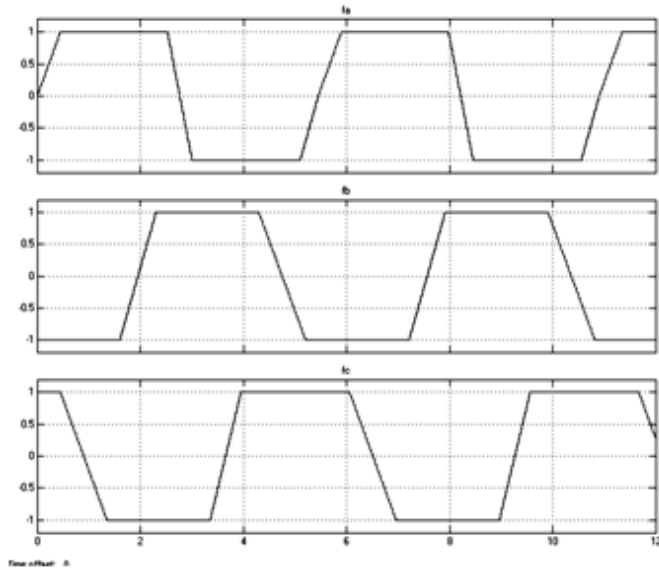


Fig.2 fa,fb,fc
PID controller outputs

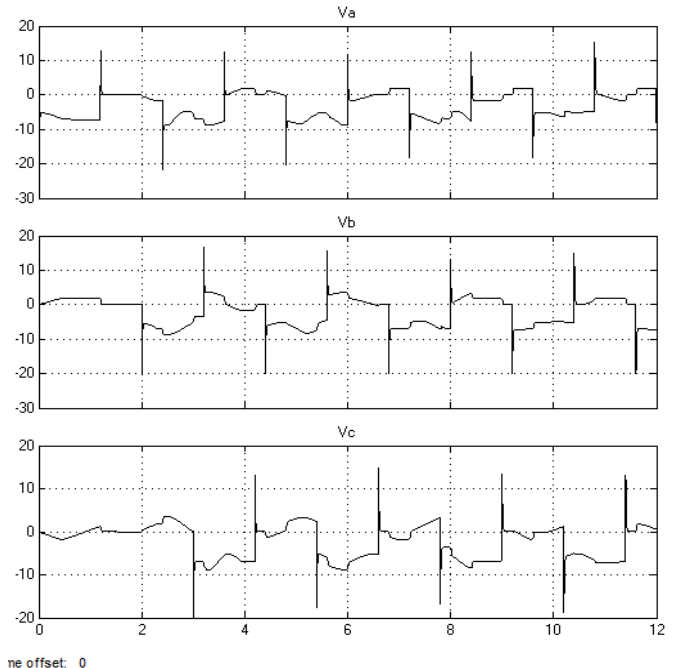


Fig.5 Voltages using PID controller

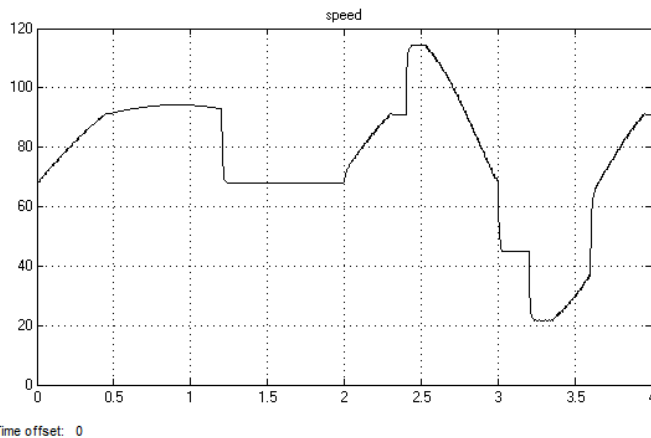


Fig.3 Speed using PID Controller

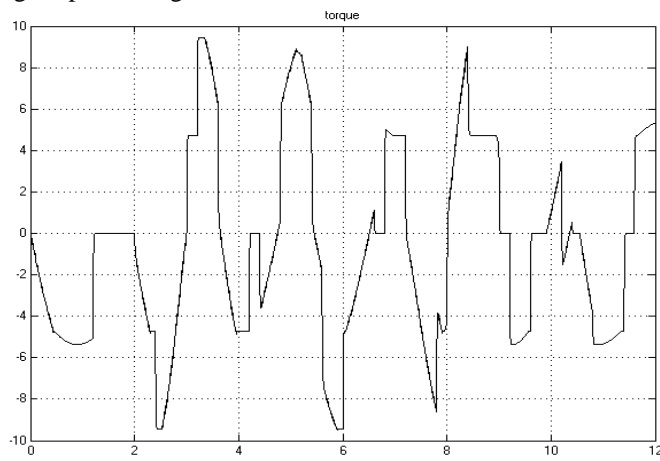


Fig.4 Torque using PID controller

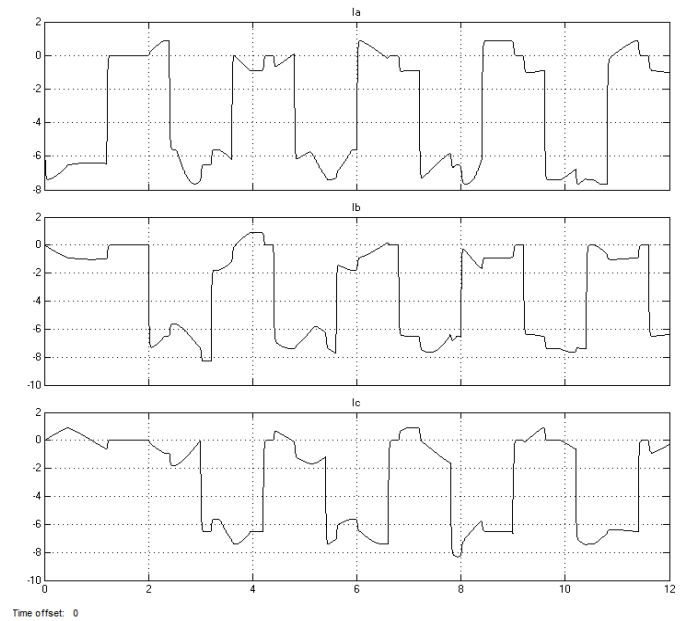


Fig.6 Current using PID controller
PWM controller outputs

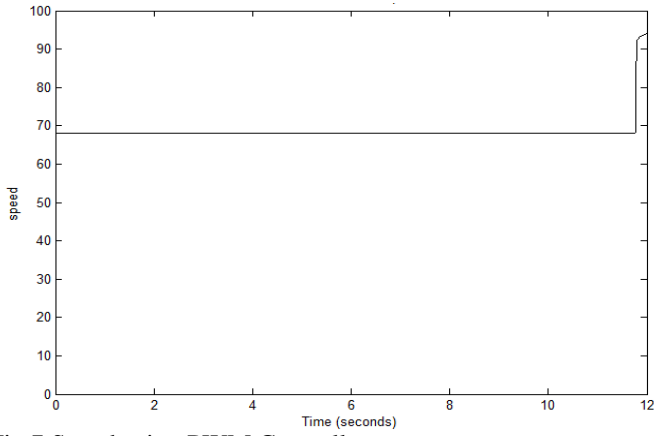


Fig.7 Speed using PWM Controller

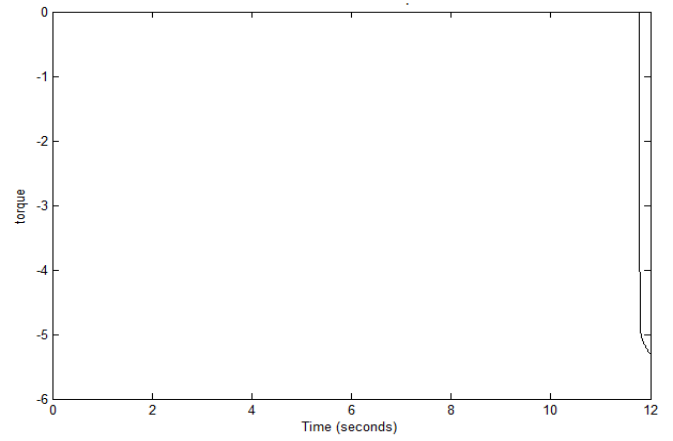


Fig.10 Torque using PWM Controller
Cascaded controller

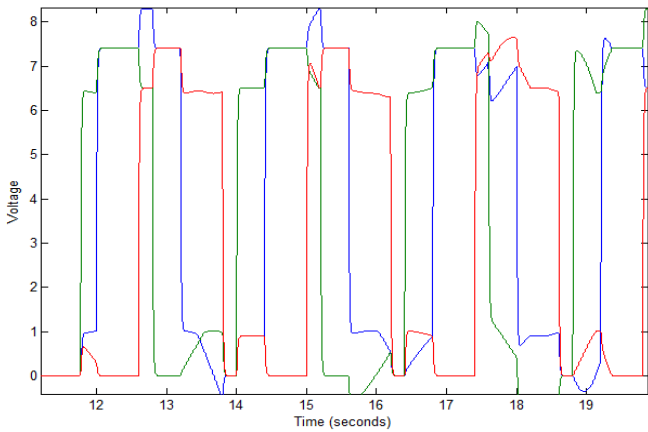


Fig.8 Voltages using PWM Controller

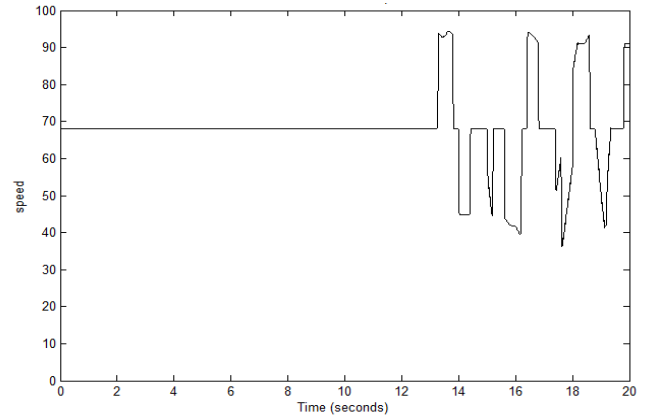


Fig.11 Speed using cascaded Controller

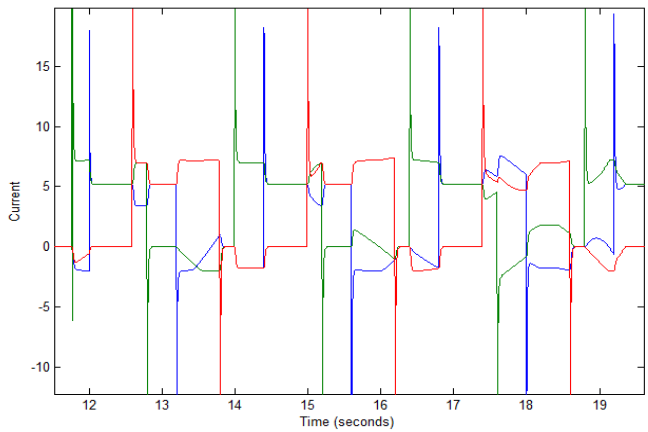


Fig.9 Currents using PWM Controller

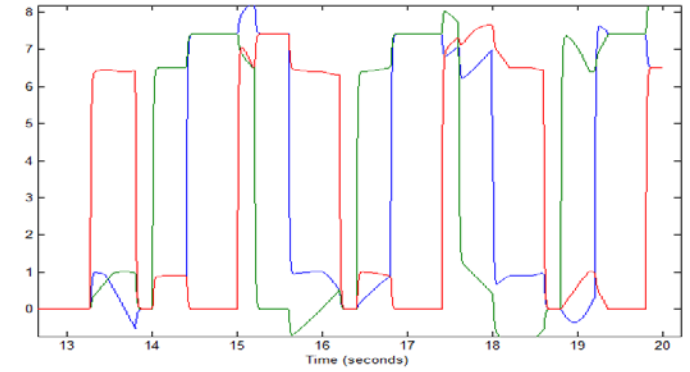


Fig.12 Voltages using cascaded Controller

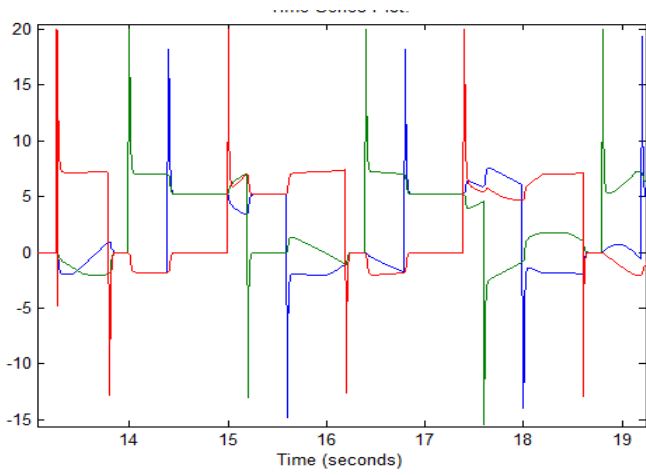


Fig.13 Currents using cascaded Controller

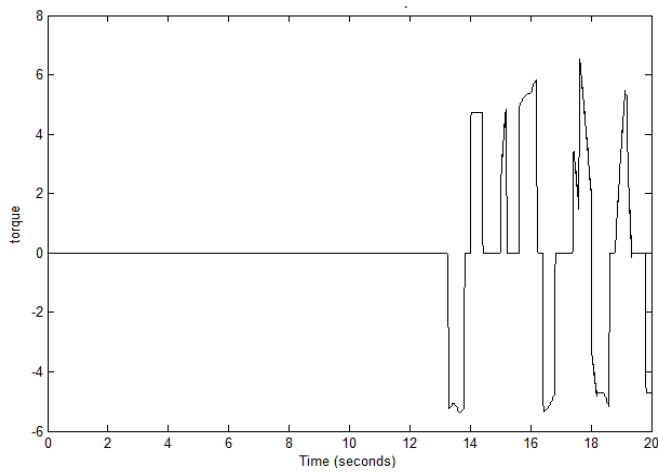


Fig.14 Torque using cascaded Controller

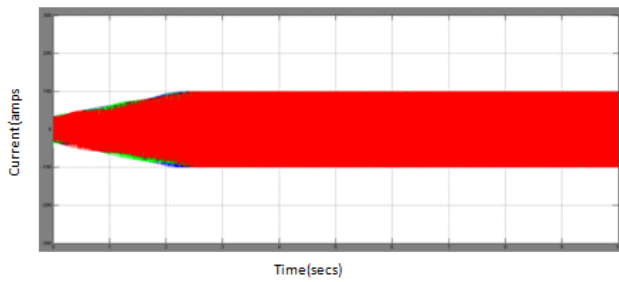


Fig.19 Output Currents of PWM controlled BLDC motor

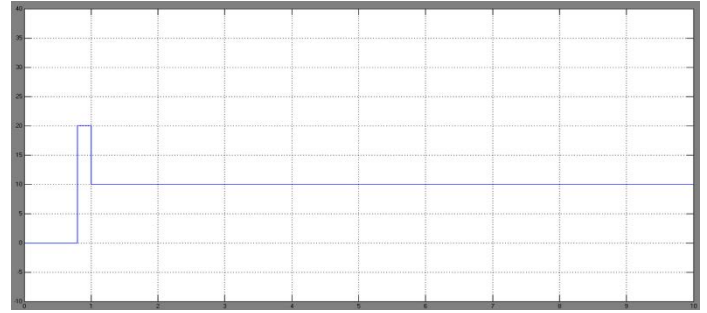


Fig.20 Electromagnetic Torque of PWM controlled BLDC motor

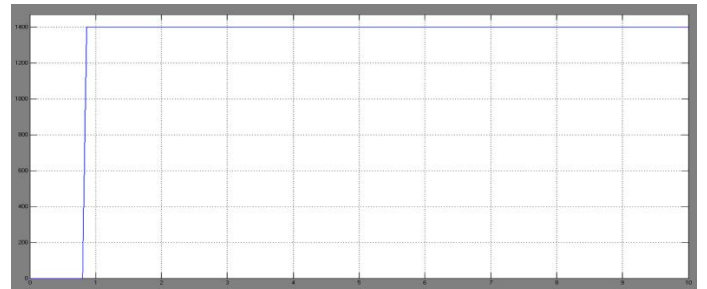


Fig.20 Speed of PWM controlled BLDC motor

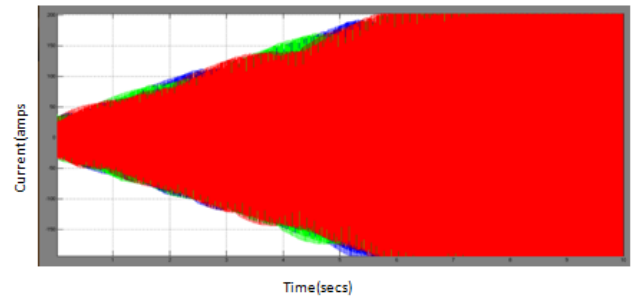


Fig.21 Output Current of cascaded controlled BLDC motor

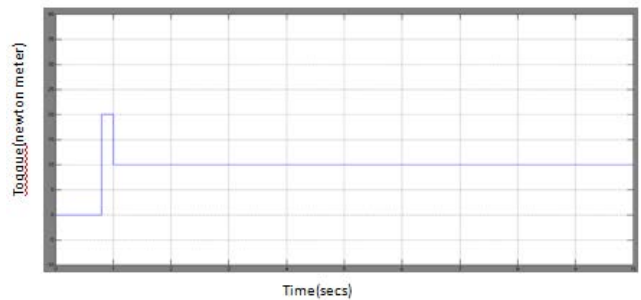


Fig.22 Electromagnetic Torque of cascaded controlled BLDC motor

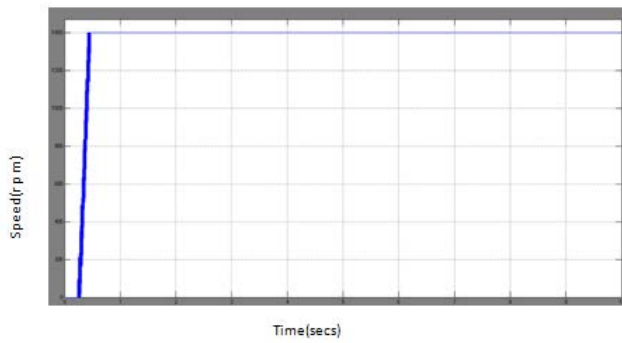


Fig23 Speed of cascaded controlled BLDC motor

Comparison of rise time, peak overshoot, peak time, settling time

Controller	Rise time (seconds)	Peak Overshoot (%)	Peak Time (seconds)	Settling time (seconds)
PI	0.0261	2.46	0.0542	0.0628
PID	0.00646	34.7	0.0203	0.0556
PWM	0.00384	73.2	0.0169	0.0552
Cascaded	0.00209	157	0.0149	0.0776

VII.CONCLUSION

In this paper, a mathematical model of BLDC motor is developed. The simulation of the permanent magnet brushless DC motor is done by using the software package MATLAB/SIMULINK.

From the simulation, the phase current , phase voltage , torque and back EMF is analyzed. A PID controller is employed for the position control of PMLDC motor. Effectiveness of the model is established by the wide range of operating conditions. The position controller has been designed for closed loop operation of PMLDC motor and the motor runs nearly to the reference position. The results are shown above using MATLAB tool and results are shown.

VIII REFERENCES

[1] H. Inaba, S. Shima, A. Ueda, T. Ando, T. Kurosawa and Y. Sakai, "A new speed control system for DC motors using GTO converter and its application to elevators," IEEE Trans. Ind. Applcat., vol. 21, pp. 391 -397, March/April 1985.

[2] M. Hombu, S..Ueda, A. Ueda and Y. Matsuda "Anew current source GTO inverter with sinusoidal output Voltage and current," IEEE Trans. Ind. Applcat., vol. 2 1, pp. 1192-1 198, Sept./Oct. 1985.

[3] H. Inaba, S. T. Nara, H. Takahashi\$M. Nakazato, "High speed elevators controlled by current source inverter system with sinusoidal input and output," Elevator World, pp. 54-60, March 1989.

[4] J. M. D. Murphy and F. G. Tumbull, Power Electronic control of AC motors, Pergamon Press, Oxford, England, 1988, pp. 306-330.

[5] Universal power analyzer PM 3000A users' manual, Voltech Instruments, Abingndon, England, 1997.

[6] S.K.Sul and T.A.Lipo, "Design and performance of a digitally based voltage controller for correcting phase," IEEE Trans on Ind. Appl., vol.26, no.3, pp. 434-440, May/June, 1990

[7] R. Uhrin and F. Profumo, "Stand alone AC/DC converter for multiple inverter applications," Power Electronics Specialists Conference, PESC '96 Record, 27th Annual IEEE, Vol. 1, pp. 120 -126, 23-27 June, 1996

[8] B. T. Ooi, Y.Guo, X.Wang, H.C. Lee, H.L. Nakra, and J.W. Dixon,

"Stability of PWM HVDC Voltage Regulator Based on Proportional-Integral Feedback," EPE Firenze'91, vol.3, pp.3-076-3-081, 1991

[9] M. Nishimoto, J.W. Dixon, A.B. Kulkarni and B.T. Ooi, "An integrated controlled-current PWM rectifier chopper link for sliding mode position control," IEEE, Ind. Appl. Soc. Annual Meeting, pp. 752-757, October, 1996

[10] M. Gaiceanu, Inverter Control for Three-Phase Grid Connected Fuel Cell Power System, Compatibility in Power Electronics, 2007. CPE '07,